Hydrodynamic studies of a 15 MW semi-submersible FOWT to assess the suitability of the inclusion of a damper system

Yu Gao, Chenyu Zhao, Lars Johanning, Ajit C Pillai

Abstract—**Floating Offshore Wind Turbines can exploit the high energy density experienced in offshore environments, with turbines now reaching up to 15 MW in size. However, given the larger size of these turbines and the environmental conditions they are exposed to, there remain significant challenges in motion stabilization. To overcome these challenges, the inclusion of a damper system could be considered to reduce motions. This paper conducts a numerical hydrodynamic study of a 15 MW semi-submersible floating offshore wind turbine under a range of environmental conditions, informing the design criteria for the damper system. The study presents both findings in the time- and frequency-domain. In the first instance the time-domain was used to determine the dominant motion characteristics. The initial study identified that the pitch motion is of main concern. As a consequence, in the frequency-domain study the focus is given to the pitch motion. Excitation modes were observed at both, eigenfrequency and excitation frequency, dependent on wave conditions. Within the discussion a dual damper system is suggested to increase stability of the platform.**

Keywords—**Floating offshore wind turbine, hydrodynamic analysis, damper system, Orcaflex.**

I. Introduction

Offshore wind power, as a clean energy resource, has presented a significant contribution to the development of energy from renewable energy sources. The attractive and competitive source has overwhelming advantages over different renewable energy technologies, including solar, tidal, and wave energy [1]. Compared to onshore wind energy, offshore wind energy, is almost three times more efficient than onshore wind energy, and are more effective due to the more consistent winds in offshore environments [2], [3]. With the continuous advancement of technology, the Offshore Wind Turbines (OWTs) have evolved to become larger in size and are now deployed in deeper sea depth. At depths beyond 50 m, bottom-fixed supporting structures cease to be economically viable [4]. As a result, floating offshore wind turbines (FOWTs) have emerged as a viable solution to harness wind power in deeper offshore areas [5]. There are four common types of FOWTs classified by the foundations: spar buoy, tensioned-leg platform (TLP), barge, and semisubmersible.

In general, the FOWT presents a significant challenge towards motion stabilization due to the severe environmental loads, including wave, wind, and current loads. These forces can cause undesirable high and low order motions [6]. The wave loads, including second-order wave loads, could excite the platform pitch resonance, which could cause structural failures [7]. Due to the turbulent aerodynamic and hydrodynamic loads, the wind turbine tower vibration can be significant and has a noticeable impact on downtime, the lifetime of the components, and even the overall integrity of the FOWT [8]. Additionally, the wind loads can be prominent in the surge, pitch motions, and tower bending moments with the increasing size of the wind turbine [9]. Therefore, it is highly important to study the motion responses of FOWTs and search for engineering solutions to eliminate undesirable motions and improve system reliability.

Multiple studies have been conducted exploring damper devices for FOWT applications [10]. Basu et al. [11] verified the effectiveness of a tuned liquid column damper (TLCD) mitigating the vibrations for monopile fixed OWT. Lackner et al. [12], [13] investigated passive

This work was supported in part by a CSC PhD Studentship.

Yu Gao is with the Renewable Energy Group, Faculty of Environment, Science, and Economy, University of Exeter, Penryn, Cornwall, UK, TR10 9FE (yg384@exeter.ac.uk).

Chenyu Zhao is with the Renewable Energy Group, Faculty of Environment, Science, and Economy, University of Exeter, Penryn, Cornwall, UK, TR10 9FE (c.zhao@exeter.ac.uk).

Lars Johanning is with the Renewable Energy Group, Faculty of Environment, Science, and Economy, University of Exeter, Penryn, Cornwall, UK, TR10 9FE (l.johanning@exeter.ac.uk).

Ajit C Pillai is with the with the Renewable Energy Group, Faculty of Environment, Science, and Economy, University of Exeter, Penryn, Cornwall, UK, TR10 9FE (a.pillai@exeter.ac.uk).

Digital Object Identifier: https://doi.org/10.36688/ewtec-2023-497

structural control of various types for 5 MW FOWTs, including barge, spar, and tension leg platforms, using a simplified model. The results showed that the tuned mass damper (TMD) is efficient in the vibration reduction of FOWTs, especially in side-to-side tower bending. Li et al. [14] implemented TMDs to reduce the vibrations of the platform and tower. The lower stiffness TMDs can dissipate the energy of platform pitch vibration, and the higher stiffness TMDs absorb the energy of tower bending. Furthermore, Hemmati et al.[15] studied the effectiveness of a combined TLCD and TMD system on the vibration reduction of OWTs. The results demonstrated that the TMDs are more efficient in operating conditions.

Active dampers are effective in reducing structural loads and vibrations but at the expense of active power and large stroke [16]. Brodersen et al. [17] employed an active tuned mass damper (ATMD) for fixed OWTs to investigate its effect on tower vibrations. The authors concluded that the ATMD is highly efficient in reducing the tower vibrations in transient conditions. Hu and He [18] investigated the active control for barge-type FOWT. In this study, the ATMD was limited by a stroke-limited hybrid mass damper. Fitzgerald et al. [19] studied the effect of an ATMD on onshore wind turbines. The results demonstrated that the ATMD presents a significant improvement in the reliability of the wind turbine at the rated speed.

This paper provides a hydrodynamic analysis of wave loading on the IEA 15 MW FOWT installed on a semi-submersible structure, focusing on the response characteristics of the moored system in order to inform the design of a suitable active or passive damper that would enhance the stability. The numerical analysis is conducted under various wave conditions using Orcaflex [20] in the time domain and frequency domain while taking into account the wave drift loads. Key response frequencies for different wave periods and heights are assessed to inform about suitable damper solutions. This paper is organized as follows: Section 2 describes the numerical model, key parameters, and environmental cases; Section 3 presents the analysis results of the time-domain and frequency-domain study; Section 4 suggests a potential damper system; and Section 5 presents the conclusion and future work.

II. NUMERICAL STUDY

A. *Governing equations*

This study employs the IEA 15 MW semi-submersible FOWT, shown in Fig. 1, designed by National Renewable Energy Laboratory, Technical University of Denmark, and University of Maine jointly. In this study the focus is given to the hydrodynamic loading and restoring forces. Therefore, the motion equation can be expressed in (1).

$$M\ddot{X}(t) + \int_{-\infty}^{t} L(t-\tau)\dot{X}(\tau)d\tau + KX(t) = F_w \qquad (1)$$

Where M is the mass matrix, consisting of the structural mass, and added mass matrix; $L(t-\tau)$ is the retardation function matrix, including frequency dependent added mass and damping terms. B is the damping matrix including viscous damping B_v causing viscous drag loads, radiation damping B_r, and structural damping B_s; K is the component of stiffness matrix which are mooring stiffness K_m, and hydrostatic stiffness K_h (hydrostatic restoring force); $\ddot{X}(t)$, $\dot{X}(t)$, $X(t)$ are acceleration, velocity, and displacement of structure respectively; F_w is the wave loads, including incident wave load and diffraction wave load.

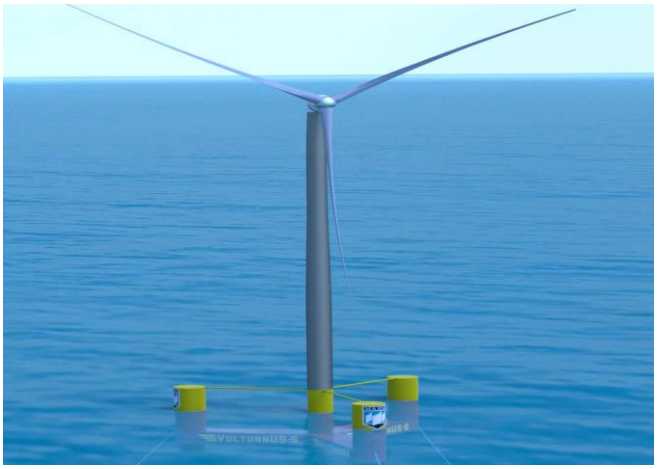

Fig. 1. The Umaine VolturnUS-S reference platform to support 15 MW win turbine [21].

In this study, the Morison equation and diffraction theory are both considered to take into account the viscous drag force [22] calculating the first-order wave loads including drag loads, incident wave loads, diffraction loads, and radiation loads. Additionally, the second-order wave loads are considered as semi-submersibles are sensitive to the second-order wave effects especially wave drift loads [7]. The second-order wave loads, proportional to the square of wave amplitude, can be divided into two parts: difference-frequency loads (wave drift loads) and sum-frequency loads. The former can cause the offshore structure to oscillate at difference-wave frequencies while latter lead an oscillating at sum-wave frequencies. However, the sum-frequency loads are excluded as they have negligible effects on the substructure according to [23].

B. *The key parameters of the FOWT*

The IEA 15 MW FOWT utilizes the UMaine VolturnUS-S reference platform, which was designed by the University of Maine specifically to support the IEA 15 MW reference wind turbine.

The key parameters of the FOWT can be seen in [24]. The platform is a steel semi-submersible with a draft of 20 m, designed for deployment in 200 m of water depth. It is held

in place by the three-line chain catenary mooring system. The total mass of the platform is 17,854 tons. The three base columns have diameters of 12.5 m and are located 51.75 m from the tower center. The elevation of the platform above sea level is 15 m.

The wind turbine system [21] consists of two separate components, the tower and the rotor and nacelle assembly (RNA). The height of the tower reaches 150 m, which allows 30 m of water surface clearance. The blade length of the reference turbine is 117 m with a root diameter of 5.2 m, and the mass of the blade is 65 tons.

The mooring system properties are presented in Table I [24]. For the mooring system, the finite element solution is adopted to calculate the loads applied by the mooring system, as it can obtain a realistic approximation with high accuracy.

TABLE I
MOORING SYSTEM PROPERTIES [24]

Parameter	Value	Unit
Type	Chain Catenary	-
Number	3	-
Anchor Depth	200	m
Fairlead Depth	14	m
Anchor Radial Spacing	837.6	m
Fairlead Radial Spacing	58	m
Nominal Chain Diameter	185	mm
Dry Line Linear Density	685	kg/m
Extensional stiffness	3,270	MN
Fairlead Pretention	2,437	kN

C. *Numerical model setup*

In Orcaflex, the semi-submersible floating structure is represented by six degrees of freedom (DOF) rigid body, connected with three pontoons. The mass of pontoons is zero as they are assumed to be built into the substructure. The floating foundation is modelled as having 6-DOF considering the effects of first-order wave loads, wave drift loads, wave drift damping and added mass. The other damping, accounting for the quadratic damping coefficients applied to the platform motions, is added in the analysis. The properties of the platform are obtained by a diffraction analysis in OrcaWave considering the full system including tower, nacelle, and rotor.

The blades and tower are modelled by the line elements. The nacelle and hub are modelled in OrcaFlex as 6-DOF buoys with mass and inertia. The tower is divided into 26 segments each measuring 5 m in length. The connection between the tower and the substructure is assumed to be rigid. The mooring lines are discretized into 85 sections each of 10 m length. The azimuth between the lines are 120 degrees. The finite element method is used to calculate the mooring loads.

In this study, the direction of the incident wave is 180 degrees heading to the wind turbine, defined by the JONSWAP spectrum with a crest factor of 3.3. The wind speed is set to zero to investigate the wave effects. The simulations are executed for 3600s with a 400-seconds build-up stage to eliminate the transit influence. The dynamic time step is 0.025s.

Newman's approximation method [7] is used to calculate the second-order wave forces. This approximation only considers the diagonal values of the full quadratic transfer function (QTF) and avoids computing the second-order velocity, which can improve the computational efficiency and, at the same time, maintain the accuracy.

D. *Natural frequencies of the FOWT*

The natural frequencies, seen in Table II, were obtained from the module of the modal analysis in Orcaflex [25], [26]. The modal analysis calculates the undamped natural modes of a system, characterised by their modal frequency and mode shape. The undamped natural modes represent that the added mass and radiation damping are neglected in this process, as it is difficult to account for the frequency dependent data.

In this study, the average added mass and radiation damping matrixes of the platform under the infinite frequency, only considering the diagonal elements, are supplied for a more accurate natural frequency calculation.

TABLE II
NATURAL FREQUENCIES OF THE FOWT

Parameter	Value	Unit
Surge	0.008	Hz
Sway	0.007	Hz
Heave	0.046	Hz
Roll	0.035	Hz
Pitch	0.036	Hz
Yaw	0.012	Hz

E. *Environmental loading cases*

The designed load cases are selected based on the 25-year measurements of Gran Canaria. The cases are selected from the measured data in Fig. 2. The higher significant wave heights (H_s) of 5.4 m, 6 m, and 7.1 m are introduced to serve as extreme wave conditions. Therefore, the range of significant wave height is 2.5 m to 7.1 m. According to Table II, the natural period of the structural pitch is approximately 28 s. Thus, an extended range of peak periods (T_p) from 4.98 s to 28 s is selected.

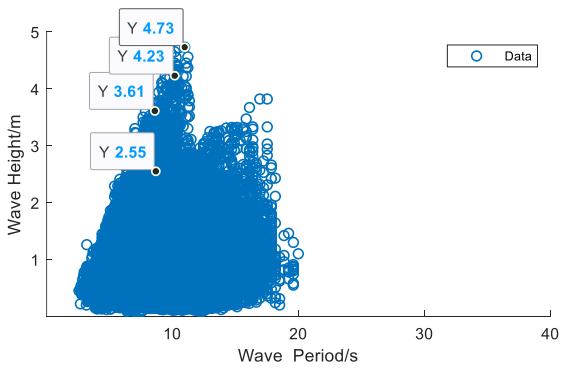

Fig. 2 25-year measured data of Gran Cranaria

The details of the cases can be found in Table III to Table V. The time-domain results of cases 1-30 determine the key motions of the FOWT in 6 DOFs. Cases 1-6 are used to investigate motion responses of the FOWT by sharing the same wave period and different significant wave heights. Similarly, cases 7-13 and 19-25 explore the wave period effects by using the same significant wave height and different wave periods.

TABLE III
DESIGN LOAD CASES WITH A RANGE OF WAVE HEIGHTS AT PERIOD 8 S

Case number	Significant wave height (m)	Periods (s)
1	2.5	8
2	3.6	8
3	4.2	8
4	5.4	8
5	6	8
6	7.1	8

TABLE IV
DESIGN LOAD CASES WITH A RANGE OF WAVE PERIODS AT SIGNIFICANT WAVE HEIGHT 4.73 M

Case number	Significant wave height (m)	Periods (s)
7	4.73	4.98
8	4.73	7.04
9	4.73	9.43
10*	4.73	11.9
11	4.73	14.29
12	4.73	16.13
13	4.73	18.87
14	4.73	20
15	4.73	23.1
16	4.73	24.6
17	4.73	26.2
18	4.73	28

TABLE V
DESIGN LOAD CASES WITH A RANGE OF WAVE PERIODS AT SIGNIFICANT WAVE HEIGHT 7.1M

Case number	Significant wave height (m)	Periods (s)
19	7.1	4.98
20	7.1	7.04
21	7.1	9.43
22	7.1	11.9
23	7.1	14.29
24	7.1	16.13
25	7.1	18.87
26	7.1	20
27	7.1	23.1
28	7.1	24.6
29	7.1	26.2
30	7.1	28

III. RESULTS

This section presents the results of the hydrodynamic analysis in time and frequency domains under different wave conditions.

F. *Time-domain results*

It is critical to identify the key motions of the FOWT before employing a damper system. Typically, the motions of the platform and wind turbine are consistent as they are assumed to be connected rigidly. Fig. 3 presents the 6 DOFs motion amplitudes of the FOWT with a range of significant wave heights at a fixed wave period of 8 s. Fig. 4 presents the 6 DOFs motion amplitudes of the FOWT with a range of wave periods at fixed significant wave heights.

The results show that the motion amplitudes of roll, yaw, and sway are always close to zero with varying significant wave heights and wave periods The surge, heave, and pitch motions are relatively more remarkable than these motions. The amplitudes of surge motion become larger with the increase in significant wave heights at fixed wave periods but smaller with the increasing of wave periods at fixed significant wave heights. The amplitudes of heave motion are not sensitive to the varying significant wave heights and wave periods compared to surge and pitch. The pitch motion amplitudes could increase dramatically under the same conditions.

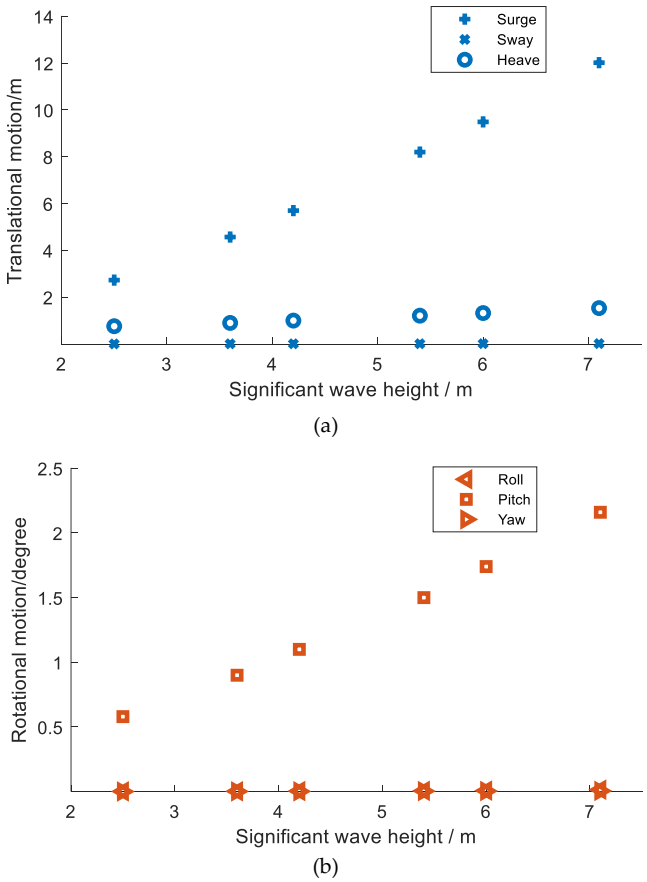

Fig. 3. Motion amplitudes in 6 DOFs under a range of significant wave heights under cases 1-6. (a) translational motions; (b) rotational motions.

According to [27], [28], the surge and heave motions can be restricted effectively by the mooring system. If the maximum offset in the surge of the platform is less than 50% of water depth then it is acceptable [29]. Generally, the

heave plate can be effective and common in reducing the heave motion responses of the FOWT [30]. Accordingly, the pitch motion is analyzed as the key parameter to be damped.

For the pitch motion, the results in Fig. 3 (b) show that the pitch motion under different significant wave heights exhibits the same trend but with different amplitudes. In Fig. 4, when the wave period is less than approximately 18 s, the amplitude of pitch motion is less affected by the change in wave period. However, the amplitude of the pitch motion becomes much larger when the wave period is more than 18s.

Based on the time-domain results, the pitch motion is determined as the key motion to be damped. The significant wave height and wave period could have a remarkable impact on the pitch motion. Therefore, the pitch motion results are then analyzed under frequency domain.

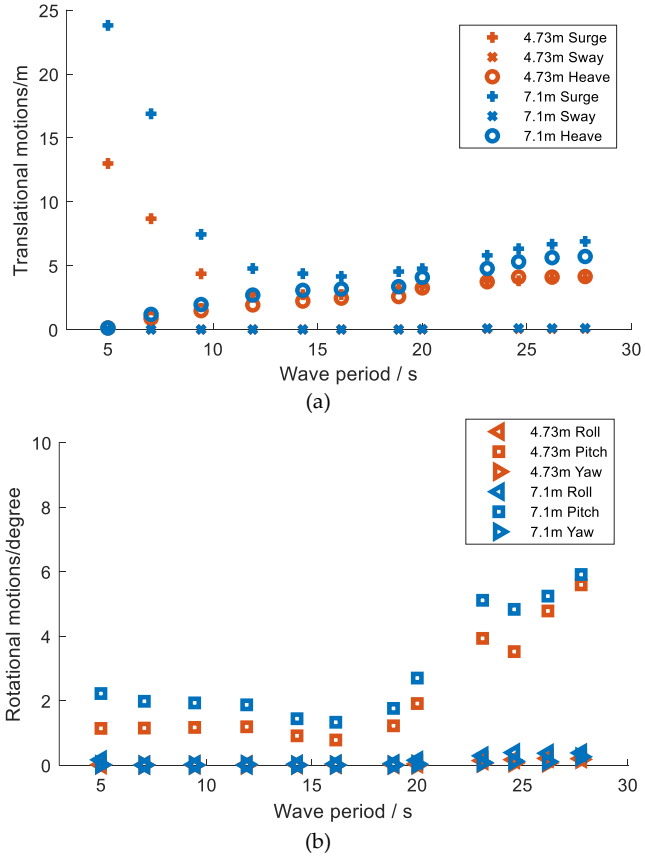

Fig. 4. Motion amplitudes in 6 DOFs under a range of wave periods at two fixed significant wave heights (4.73 m and 7.1 m) under cases 7-30. (a) translational motions; (b) rotational motions.

G. *Frequency-domain results*

Fig. 5 presents the significant wave height effects on the pitch motion of cases 1-6 under fixed wave period of 8 s, Table III. The results indicate that there are two dominant peaks in the power spectral density plots. The first peak is at the low frequency region (<0.05), whilst the second peak is at the high frequency region (>0.05). The two peaks become more prominent when significant wave height increases. Additionally, the two peaks are almost equal in energy, particularly when the significant wave height is 7.1 m. The first peak occurs at the natural frequency of the structural pitch motion, whilst the second peak is around the wave frequency, which means it is induced by the first-order wave loads. The increasing significant wave heights have no influence on the frequencies of the two peaks.

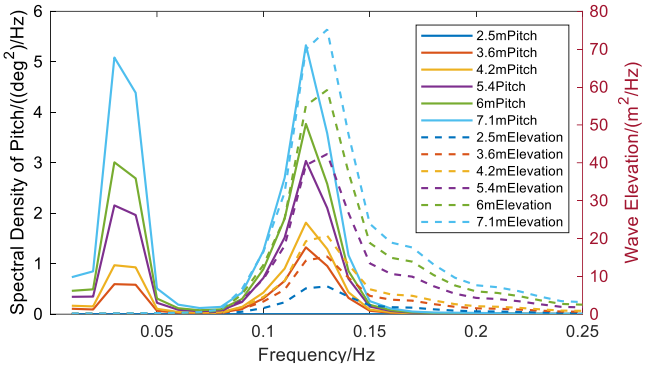

Fig. 5. Variation in pitch motion of spectral density with a range of significant wave heights at a fixed wave period of 8 s.

Fig. 6 shows the results of the pitch spectral density under considering second-order wave effects and without second-order wave effects to identify the cause of the first peak. It is observed that there is no first peak at the low frequency region without considering the second-order wave loads. Only one case is shown, as other cases are similar. This indicates that the first peak is induced by the second-order wave loads (wave drift loads).

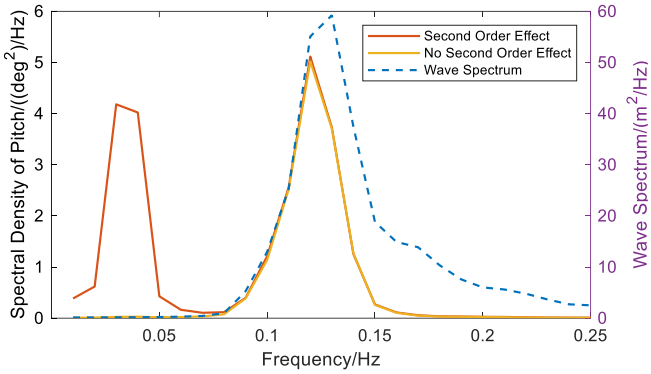

Fig. 6. Comparison of the spectral density of pitch motion with considering the second-order wave effects under case 19.

Fig. 7 shows the results of the two peaks with the change in the wave period under fixed significant wave heights. As illustrated in Fig. 5, the spectral density peak frequencies show no difference with the varying significant wave heights. Therefore, only the results of a significant wave height of 4.73 m are presented (cases 7-18). The comparison of the spectral density of pitch motion under different significant wave heights is shown in the following.

In Fig. 7 (a), the results show that the frequencies of the first peak remain at the natural frequency of pitch motion, and the second peak frequencies gradually approach the natural frequency with the increase in the wave period. Notably, the frequencies between the two peaks are equal when the wave period is 18.87 s. The second peak occurs at the natural frequency of the pitch motion and there is no

original first peak. According to Fig. 7 (b), the first peak is much larger when the wave periods are 4.98 s and 18.87 s. Especially the first peak corresponding to the 18.87 s wave period is much higher than other peaks, which is caused by the resonance mode. The spectral density of the first and second peaks is close when the wave period is 7.04 s to 16.13 s.

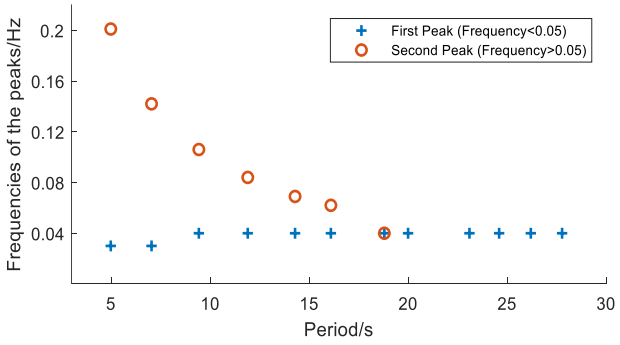

(a)

ave

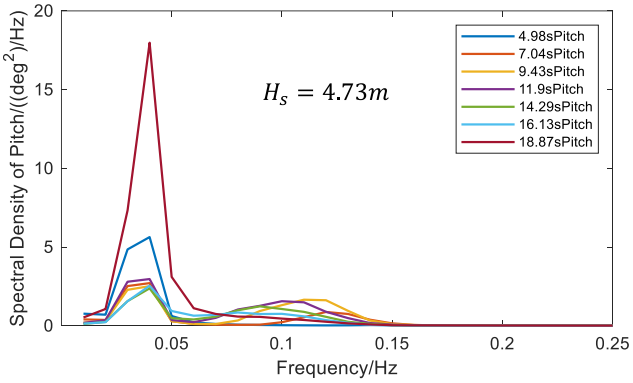

(b)

Fig. 7. Spectral density of pitch motion with a range of wave periods at fixed significant wave heights (H_s = 4.73 m). (a) Spectral density peak frequencies (wave periods from 4.98s to 28s); (b) Spectral density amplitude (wave periods from 4.98s to 18.87s).

To elucidate the relevant frequencies and the impact of the varying wave period, the two peaks in Fig. 5 and Fig. 7 are separated by replotting the graphs. More periods (13.1 s, 15.15 s and 17.54 s) are introduced between 4.98 s and 18.87 s to get greater granularity. Fig. 8 shows the first and second peaks in relation to the change in the wave period under fixed significant wave heights.

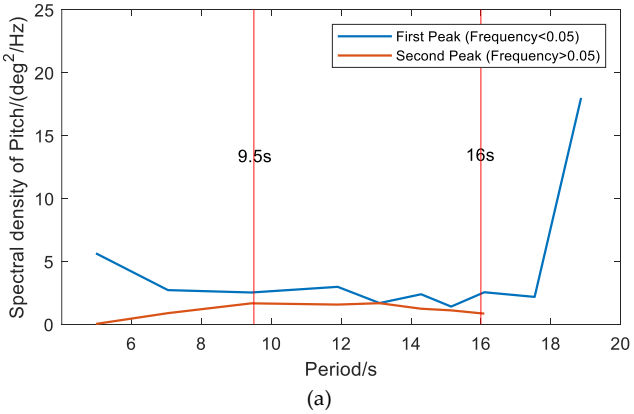

(a)

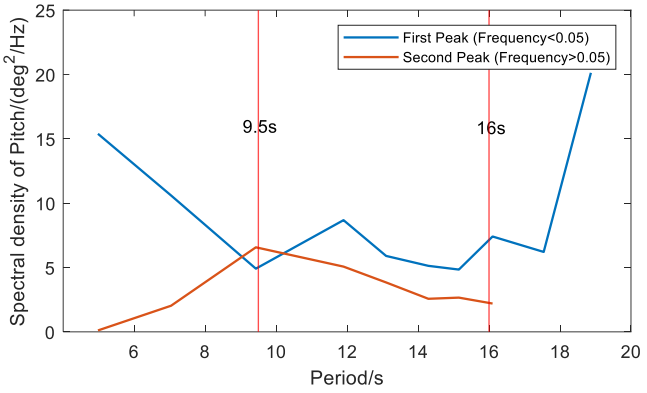

(b)

Fig. 8. Variation of the first and second peaks with a range of wave periods (4.98s to 18.87s) at fixed significant wave heights. (a) $H_s = 4.73m$; (b) $H_s = 7.1m$.

It is apparent that the pitch motion of spectral density under the two wave heights has almost the same trend. The first peak could dominate during the wave period a range between 4.98 s to 18.87 s. The second peak shows a trend of increasing and then decreasing with the increase of the wave period, which reaches the maximum value at the wave period of 9.43 s. As the significant wave height increases to 7.1 m, the first and second peaks become much higher.

There are three areas identified in the two figures. In the first area (wave period less than 9.5 s), the first peak shows a downward trend while the second peak increases. Meanwhile, the first peak is much larger than the second peak. In the second area (wave period between 9.5s and 16s), the changes of the first and second peaks are not significant according to the change in the wave period, similar to the results of Fig. 4 (b). In addition, the first and second peak are almost equal in this area. A difference between the two figures in this area is that the second peak could be larger than the first peak when the significant wave height is 7.1 m. In the third area (wave period more than 16s), the first peak increase dramatically with the increasing wave period. There is only the first peak in this area, similar to Fig. 7 (a).

The frequency-domain results demonstrate that there are two dominant spectral density peaks of the pitch motion. The two peaks occur at different frequencies. The first peak, induced by second-order wave loads, is at the natural frequency of pitch motion. The second peak, induced by the first order wave force, is related to the wave frequency. Moreover, the first peak is dominant compared to the second peak especially in the first and third areas.

IV. DISCUSSIONS

This paper performed hydrodynamic analysis of the FOWT to discuss the necessity of introducing the damper system. The results are presented both in time and frequency domains.

Based on the time-domain results, the motion response of the FOWT is analyzed. The previous studies show that the damper system is commonly installed in the nacelle of

the wind turbine or the platform. The slight motion difference might be between the platform and the wind turbine. This is because the tower is modelled using a line element with high stiffness in Orcaflex. In this study, the damper system will be considered to be installed in the nacelle and the platform, respectively, to enhance the stability of the structure.

The results shown in Fig. 3 and Fig. 4 determine the pitch motion to be damped by employing a damper system. For the FOWT, the tower can exceed 100 m in height. Even small pitch motions can cause a critical dynamic effect which leads to worse excursions in the tower [6].

The motion of roll, yaw, and sway can be ignored because the excitation at these motions might be considerably not significant with the wave heading towards the wind turbine. However, when the incident wave direction changes, other motions, such as roll, might become critical [31]. Therefore, a dual or multiple-damper system, consisting of more than one damper, each acting in a single-direction, may be required [13], [31]. From the results of Fig. 3 and Fig. 4, the significant wave height plays a crucial role in the motion amplitude of pitch as the pitch motion amplitude increases remarkably when the significant wave height becomes higher. Besides, the wave period could excite the significant amplitude of pitch motion. This is because the wave period is close to the natural period of pitch motion.

Based on the frequency-domain results, two dominant peaks in the spectral density plots are identified at low and high frequency regions, respectively. According to Fig. 5-Fig. 7, the first peaks are induced by the loads at the natural frequency, leading to structural resonance. Even small second-order hydrodynamic loads may cause a significant resonant effect, which plays a crucial role in the global response of the semi-submersible [32]. The second peaks occur around the wave frequency induced by the first-order wave loads. The two components contribute to the pitch motion in Fig. 4 (b).

Fig. 8 exhibits that the first peak is higher than the second peak, especially in the first and third areas. Notably, only the first peak, induced by the first-order wave loads, is in the third area. This may be because the wave frequency is close to the natural frequency of pitch motion, and the frequency of difference frequency loads is not within the range which can excite the structural motion.

Similarly, according to Fig. 7 (a), the focus should be given to the natural frequency of the pitch motion when the wave period is larger than 18.87s. For this particular case, the single damper system may be effective and economical in motion reduction. As for the single damper system, the natural frequency of the device is tuned to the natural frequency of the structural motion to maximize energy absorption, which is the most important aspect of designing the damper system [16]. However, the results also indicate that the second peak could be close to or larger than the first peak. Overall, both the first and second peaks have a significant effect on the stabilization of the wind turbine. Based on these observations, the dual damper system is proposed as an effective and generally applicable strategy to reduce both the resonance at the natural frequency and oscillations at the wave frequency.

V. CONCLUSIONS

In this paper, the hydrodynamic analysis of the IEA 15 MW semi-submersible FOWT has been conducted under a range of wave conditions to demonstrate the requirements of the damper system. The environmental loadings are obtained from the 25-year Met Ocean data of Gran Canaria. The simulation results are presented in the time- and frequency- domain under different wave conditions. The time-domain results indicate that the pitch is the key motion required to be damped. Accordingly, the results of pitch motion are analysed further in the frequency domain. The main conclusions are summarized as follows.

- Two dominant peaks of spectral density are identified under different wave conditions.
- The first peak, related to the pitch natural frequency, is induced by the difference frequency loads. The second peak, occurring around the wave frequency, is caused by the first-order wave loads. The first peak is higher than the second peak when the wave period varies.
- A dual or multi-damper system is suggested to be employed for better motion stabilization of the structure.

The results of the hydrodynamic analysis in this paper can be the basis for applying the damper system, such as the passive and active damper.

Future work will include the wind loads to study the effects of aerodynamics on the global motion responses and two peaks. In addition, the damper solution will be studied, starting with investigating a passive damper system, including both single and dual damper systems. The study will include the method of introducing the damper system to Orcaflex. The results of this study will be used to evaluate the efficiency of the damper system. For better applicability and effectiveness of the damper system, the multiple directions and active damper systems will be investigated subsequently.

REFERENCES

[1] P. Zhang *et al.*, 'Dynamic Response of Articulated Offshore Wind Turbines under Different Water Depths', *Energies*, vol. 13, no. 11, p. 2784, Jun. 2020, doi: 10.3390/en13112784.

[2] A. Jamalkia, M. M. Ettefagh, and A. Mojtahedi, 'Damage detection of TLP and Spar floating wind turbine using dynamic response of the structure', *Ocean Eng.*, vol. 125, pp. 191–202, Oct. 2016, doi: 10.1016/j.oceaneng.2016.08.009.

[3] E. Uzunoglu and C. Guedes Soares, 'On the model uncertainty of wave induced platform motions and mooring loads of a semisubmersible based wind turbine', *Ocean Eng.*, vol. 148, pp. 277–285, Jan. 2018, doi: 10.1016/j.oceaneng.2017.11.001.

[4] A. Myhr, C. Bjerkseter, A. Ågotnes, and T. A. Nygaard, 'Levelised cost of energy for offshore floating wind turbines in a life cycle perspective', *Renew. Energy*, vol. 66, pp. 714–728, Jun. 2014, doi: 10.1016/j.renene.2014.01.017.

[5] K. C. Tong, 'Technical and economic aspects of a floating offshore wind farm', *J. Wind Eng. Ind. Aerodyn.*, vol. 74–76, pp. 399–410, Apr. 1998, doi: 10.1016/S0167-6105(98)00036-1.

[6] A. Nazokkar and R. Dezvareh, 'Vibration control of floating offshore wind turbine using semi-active liquid column gas damper', *Ocean Eng.*, vol. 265, p. 112574, Dec. 2022, doi: 10.1016/j.oceaneng.2022.112574.

[7] L. Zhang, W. Shi, M. Karimirad, C. Michailides, and Z. Jiang, 'Second-order hydrodynamic effects on the response of three semisubmersible floating offshore wind turbines', *Ocean Eng.*, vol. 207, p. 107371, Jul. 2020, doi: 10.1016/j.oceaneng.2020.107371.

[8] S. Sarkar and B. Fitzgerald, 'Vibration control of spar-type floating offshore wind turbine towers using a tuned mass-damper-inerter', *Struct. Control Health Monit.*, vol. 27, no. 1, Jan. 2020, doi: 10.1002/stc.2471.

[9] Z. Zhao, X. Li, W. Wang, and W. Shi, 'Analysis of Dynamic Characteristics of an Ultra-Large Semi-Submersible Floating Wind Turbine', *J. Mar. Sci. Eng.*, vol. 7, no. 6, Art. no. 6, Jun. 2019, doi: 10.3390/jmse7060169.

[10] S. Park, M. A. Lackner, P. Pourazarm, A. Rodríguez Tsouroukdissian, and J. Cross-Whiter, 'An investigation on the impacts of passive and semiactive structural control on a fixed bottom and a floating offshore wind turbine', *Wind Energy*, vol. 22, no. 11, pp. 1451–1471, 2019, doi: 10.1002/we.2381.

[11] S. Colwell and B. Basu, 'Tuned liquid column dampers in offshore wind turbines for structural control', *Eng. Struct.*, vol. 31, no. 2, pp. 358–368, Feb. 2009, doi: 10.1016/j.engstruct.2008.09.001.

[12] M. A. Lackner and M. A. Rotea, 'Passive structural control of offshore wind turbines', *Wind Energy*, vol. 14, no. 3, pp. 373–388, Apr. 2011, doi: 10.1002/we.426.

[13] G. Stewart and M. Lackner, 'Offshore Wind Turbine Load Reduction Employing Optimal Passive Tuned Mass Damping Systems', *IEEE Trans. Control Syst. Technol.*, vol. 21, no. 4, pp. 1090–1104, Jul. 2013, doi: 10.1109/TCST.2013.2260825.

[14] C. Li, T. Zhuang, S. Zhou, Y. Xiao, and G. Hu, 'Passive Vibration Control of a Semi-Submersible Floating Offshore Wind Turbine', *Appl. Sci.*, vol. 7, no. 6, Art. no. 6, Jun. 2017, doi: 10.3390/app7060509.

[15] A. Hemmati, E. Oterkus, and M. Khorasanchi, 'Vibration suppression of offshore wind turbine foundations using tuned liquid column dampers and tuned mass dampers', *Ocean Eng.*, vol. 172, pp. 286–295, Jan. 2019, doi: 10.1016/j.oceaneng.2018.11.055.

[16] D. Villoslada, M. Santos, and M. Tomás-Rodríguez, 'TMD stroke limiting influence on barge-type floating wind turbines', *Ocean Eng.*, vol. 248, p. 110781, Mar. 2022, doi: 10.1016/j.oceaneng.2022.110781.

[17] M. L. Brodersen, A.-S. Bjørke, and J. Høgsberg, 'Active tuned mass damper for damping of offshore wind turbine vibrations: Active tuned mass damper for damping of offshore wind turbine vibrations', *Wind Energy*, vol. 20, no. 5, pp. 783–796, May 2017, doi: 10.1002/we.2063.

[18] Y. Hu and E. He, 'Active structural control of a floating wind turbine with a stroke-limited hybrid mass damper', *J. Sound Vib.*, vol. 410, pp. 447–472, Dec. 2017, doi: 10.1016/j.jsv.2017.08.050.

[19] B. Fitzgerald, S. Sarkar, and A. Staino, 'Improved reliability of wind turbine towers with active tuned mass dampers (ATMDs)', *J. Sound Vib.*, vol. 419, pp. 103–122, Apr. 2018, doi: 10.1016/j.jsv.2017.12.026.

[20] 'OrcaFlex Help'. https://www.orcina.com/webhelp/OrcaFlex/ (accessed May 14, 2023).

[21] E. Gaertner *et al.*, 'Definition of the IEA 15-Megawatt Offshore Reference Wind Turbine', National Renewable Energy Laboratory (NREL), Report, 2020.

[22] Z. Cheng, H. A. Madsen, Z. Gao, and T. Moan, 'A fully coupled method for numerical modeling and dynamic analysis of floating vertical axis wind turbines', *Renew. Energy*, vol. 107, pp. 604–619, Jul. 2017, doi: 10.1016/j.renene.2017.02.028.

[23] S. Gueydon, T. Duarte, and J. Jonkman, 'Comparison of Second-Order Loads on a Semisubmersible Floating Wind Turbine', in *Volume 9A: Ocean Renewable Energy*, San Francisco, California, USA: American Society of Mechanical Engineers, Jun. 2014, p. V09AT09A024. doi: 10.1115/OMAE2014-23398.

[24] C. Allen *et al.*, 'Definition of the UMaine VolturnUS-S Reference Platform Developed for the IEA Wind 15-Megawatt Offshore Reference Wind Turbine', NREL/TP--5000-76773, 1660012, MainId:9434, Jul. 2020. doi: 10.2172/1660012.

[25] Z.-F. Fu and J. He, *Modal Analysis*. Elsevier, 2001.

[26] 'Modal analysis: Theory'. https://www.orcina.com/webhelp/OrcaFlex/Content/html/Modalanalysis,Theory.htm (accessed May 19, 2023).

[27] Z. Liu, Q. Zhou, Y. Tu, W. Wang, and X. Hua, 'Proposal of a Novel Semi-Submersible Floating Wind Turbine Platform Composed of Inclined Columns and Multi-Segmented Mooring Lines', *Energies*, vol. 12, no. 9, p. 1809, May 2019, doi: 10.3390/en12091809.

[28] B. Liu and J. Yu, 'Effect of Mooring Parameters on Dynamic Responses of a Semi-Submersible Floating Offshore Wind Turbine', *Sustainability*, vol. 14, no. 21, p. 14012, Oct. 2022, doi: 10.3390/su142114012.

[29] F. Lemmer, '7.5 Guidance on platform and mooring line selection, installation and marine operations'.

[30] L. Zhang, W. Shi, Y. Zeng, C. Michailides, S. Zheng, and Y. Li, 'Experimental investigation on the hydrodynamic effects of heave plates used in floating offshore wind turbines', *Ocean Eng.*, vol. 267, p. 113103, Jan. 2023, doi: 10.1016/j.oceaneng.2022.113103.

[31] V.-N. Dinh and B. Basu, 'Passive control of floating offshore wind turbine nacelle and spar vibrations by multiple tuned mass dampers: PASSIVE CONTROL OF FLOATING WIND TURBINES BY MTMDs', *Struct. Control Health Monit.*, vol. 22, no. 1, pp. 152–176, Jan. 2015, doi: 10.1002/stc.1666.

[32] A. J. Couling, A. J. Goupee, A. N. Robertson, and J. M. Jonkman, 'Importance of Second-Order Difference-Frequency Wave-Diffraction Forces in the Validation of a Fast Semi-Submersible Floating Wind Turbine Model: Preprint', National Renewable Energy Lab. (NREL), Golden, CO (United States), NREL/CP-5000-57697, Jun. 2013. doi: 10.1115/OMAE2013-10308.